JPE 19-2-21

https://doi.org/10.6113/JPE.2019.19.2.560
ISSN(Print): 1598-2092 / ISSN(Online): 2093-4718

Research on Carried-Based PWM with Zero-Sequence Component Injection for Vienna Type Rectifiers

Hui Ma†, Mao Feng*, Yu Tian*, and Xi Chen*

†,*College of Electrical Engineering and New Energy, China Three Gorges University, Yichang, China

Abstract

This paper studies the inherent relationship between currents and zero-sequence components. Then a precise algorithm is proposed to calculate the injected zero-sequence component to control the DC-Link neutral-point voltage balance, which can result in a more efficient and flexible neutral point voltage balance with a desirable performance. In addition, it is shown that carried-based PWM with the calculated zero-sequence component scheme can be equivalent to space-vector pulse-width modulation (SVPWM). Based on the proposed method, the optimal zero-sequence component of the feasible modulation indices is analyzed. In addition, the unbalanced load limitation of the DC-Link neutral-point voltage balance control is also revealed. Simulation and experimental results are shown to verify the validity and practicality of the proposed algorithm.

Key words: DC-link neutral-point voltage balance, Carried-based PWM, Vienna -type rectifier, Zero-sequence component

I. INTRODUCTION

In the past two decades, there has been a lot of research done on Vienna-type rectifier systems, including state-space averaging model derivation and control scheme development [6]-[10]. The performance of a Vienna-type rectifier depends a lot on its modulation techniques. These techniques can generally be classified into two categories: carrier-based PWM and space vector modulation (SVM). These two seemingly very different types of modulation methods have been extensively studied and widely used in different application areas. There is no clear agreement as to which modulator is better. The former is more efficient and flexible. However, it has a worse harmonic performance. Meanwhile, the latter can increase both the utilization of dc voltage and the quality of three-phase current. It can also solve the problem of unbalanced neutral point voltage by adjusting the dwell time of the redundant short vectors [11], [12]. However, it has a high computational burden due to sector identification, and the sequence table according to the sectors.

Manuscript received Aug. 19, 2018; accepted Dec. 25, 2018
Recommended for publication by Associate Editor Yun Zhang.
†Corresponding Author: mahuizz119@126.com
Tel: +86-13687274873, China Three Gorges University
*Col. Electr. Eng. & New Energy, China Three Gorges Univ., China

Scholars have developed several methods to make two modulations equivalent for three-level Vienna-type rectifiers [5], [13], [16]. One type of Vienna-type rectifier topology family is presented in Fig. 1. It consists of a main diode bridge and three bidirectional switching units, which are determined by both the switch state and the current direction. The injected zero-sequence components for a Vienna rectifier are not the same as those of the equivalent PWM method for the traditional three-level topology [10], [14], [15]. Rixin et.al. proposed a simple carrier-based PWM that is injected with proper third harmonics, and designed a DC-link neutral-point voltage balance control loop, without analyzing the voltage balancing ability [13]. In [16], the zero-sequence component is attained by exploiting the equivalence between NPC and two-level converters, where the realization of SVM is indirect and the equivalence between SVM and carrier-based PWM is not clear. In [5], equivalent carrier-based PWM is deduced based on the separated sectors and sub-sectors in static coordinates. This method does not discuss the inherent reasons for the DC-Link neutral-point voltage unbalance.

This paper is divided into six sections. Section I briefly introduces the advantages of the Vienna-type topology and discusses the SVM and carrier-based PWM for Vienna-type rectifiers. Section II describes the operation and configuration

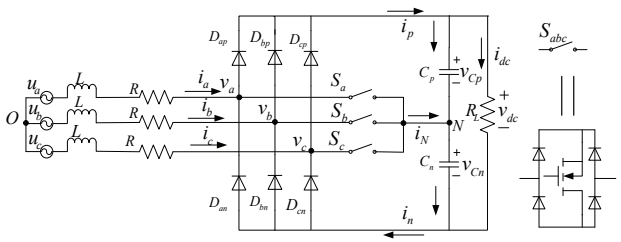

Fig. 1. Circuit schematic of a Vienna-type rectifier topology.

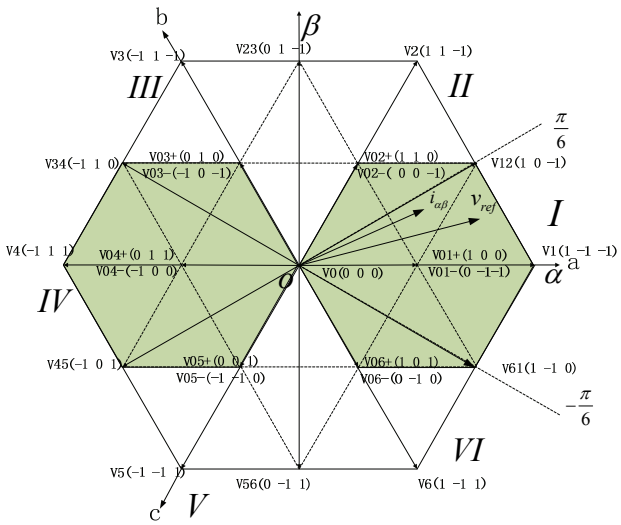

Fig. 2. Space vector diagram and six sectors of a Vienna-type rectifier.

of the Vienna-type rectifier based on SVM. Section III describes the zero-sequence component, which is injected into the carrier-based PWM to make it equal to the SVM scheme. Section IV presents a comprehensive analysis of the relationship between the DC-Link neutral-point potential variation and an average current flowing into or out of the neutral point. It is shown that the neutral current is an important variation. In other words, once the neutral current is known, the DC-Link neutral-point potential variation can be obtained. Simulation results are demonstrated in Section V. Section VI presents some conclusions.

II. Operation and Configuration of the Vienna Rectifier Based on SVM

A. SVM-based Control Strategy

Fig. 2 shows a space vector diagram and six sectors. These vectors have one zero state and 24 active states. The active states can be grouped into three categories: short vectors, medium vectors, and long vectors, the lengths of which are supposed to be normalized by Vdc, i.e. $1/3$, $\sqrt{3}/3$ and $2/3$. The six sectors are created, depending on the sector where the line current vector $i_{\alpha\beta}$ lies on the $\alpha-\beta$ plane [7]. A total of six possible sectors exist, {I, II …VI}, which activate six different

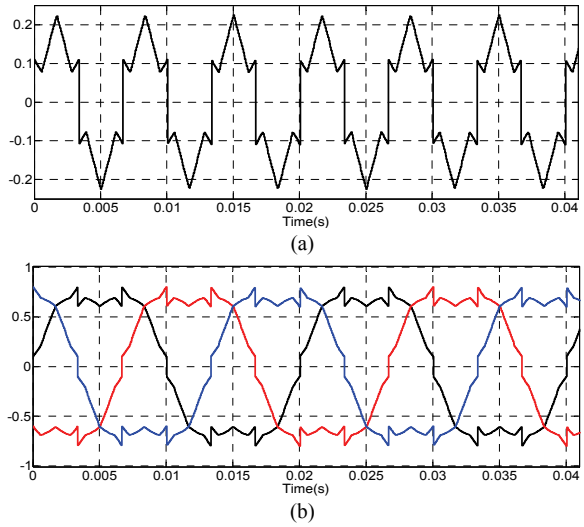

Fig. 3. Graphs of: (a) Zero-sequence component. (b) Three SVM-equivalent phase modulation waves (r=0.5, m=0.78).

set of space vectors forming a hexagonal region [7] [13]. Take sector I of $-\pi/6 \sim \pi/6$ as an example, as shown in the left shaded area in Fig. 2. It is given that the instantaneous polarity of the input currents is perfectly synchronized with the grid voltage. Due to current polarity restrictions, only the switch states of [0 0 -1] and [0 -1 0] can be realized.

B. SVM Equivalent in Carrier-Based PWM

In the sector I, phase A is in the positive period, and phases B and C are in the negative period. As shown in Fig. 2, the target vector v_{ref} is synthesized by the basic vectors of $v_{01}(v_{01+}, v_{01-})$, v_1 and v_{12}. In addition, the sequence of states applied during a switching cycle have two forms:

$$v_{01+} - v_{12} - v_1 - v_{01-} - v_{01-} - v_1 - v_{12} - v_{01+} \quad (1)$$

$$v_{01-} - v_1 - v_{12} - v_{01+} - v_{01+} - v_{12} - v_1 - v_{01-} \quad (2)$$

Since the redundant vector v_{01} has two switching state realizations, as shown in Fig. 2, namely v_{01+} and v_{01-}, and the volt-second balance for a Vienna-type rectifier considering the dc-link neutral-point voltage balance can be expressed as:

$$rT_{01}v_{01-} - T_1v_1 - T_{12}v_{12} - (1-r)T_{01}v_{01+} = \frac{T_s}{2}v_{ref} \quad (3)$$

$$rv_{01-} = (1-r)v_{01+} \quad (4)$$

where r is the time ratio of the redundant vector, which means that the ratio of the dwell time is assigned to the switching combination and injects current into the midpoint of the output capacitors. In addition, T_s is the sampling period. Substitute the Clarke transform into (3), and use $T_{01}+T_1+T_{12}=T_s/2$ and (4). Then the zero-sequence component v_z can be deduced as:

$$v_z = 2r - v_c + r(v_c - v_a) - 1 \quad (5)$$

where v_a and v_c are modulation waves.

The calculation of zero-sequence components is the same when the vectors are located in the other sectors. Therefore, the injected zero-sequence components are shown as:

$$v_z = r(1-\sigma_{\max}+\sigma_{\min})-\sigma_{\min}$$
$$\sigma_{a,b,c} = \begin{cases} v_{a,b,c} & v_{a,b,c} \geq 0 \\ v_{a,b,c}+1 & v_{a,b,c} < 0 \end{cases} \quad (6)$$

Fig. 3 shows three-phase modulation waves injected with zero-sequence component and the zero-sequence component.

III. Analysis and Calculation of Neutral-Current and Zero-Sequence Components

It is known that selecting redundant switching states and adjusting the dwell time in SVM is the process for deciding the zero-sequence component. The neutral current is an important reason for neutral-point voltage variations. If the relation for a Vienna-type rectifier is well not understood, there is confusion among practicing engineers. Therefore, it is important to build a nonlinear and discontinuous relationship between the neutral current and the zero-sequence component. Fig. 4 shows the division of six sectors diagram of a Vienna-type rectifier. In order to simplify the analysis for the Vienna-type rectifier, several assumptions are made here. The angle introduced by the input inductance between the grid side and the switch side can be ignored. The modulation frequency is higher than the output fundamental frequency, and the phase currents can be considered to be constant in a modulation period.

In section II, it is known that the lengths of these vectors are supposed to be normalized by Vdc, i.e. $1/3$, $\sqrt{3}/3$ and $2/3$. In order to conveniently analyze the zero-sequence component, the modulation index is defined here as $m=\sqrt{3}V_{ref}/V_{dc}$, where V_{dc} is defined as the dc-link output voltage, and V_{ref} is the reference voltage, achieved after a Clarke transform, in the $\alpha-\beta$ coordinate system [17]. The three phase sinusoidal modulation waves can be obtained as:

$$v_{a0} = m\cos\omega t$$
$$v_{b0} = m\cos(\omega t-2\pi/3) \quad (7)$$
$$v_{c0} = m\cos(\omega t+2\pi/3)$$

where ω is the fundamental angular frequency, and $0 \leq m \leq 2/\sqrt{3}$ (if$V_{ref}=2V_{dc}/3$then$m=2/\sqrt{3}$). In addition, two modulation regions in a space vector representation for a three-level SVM implementation are shown in Fig. 5.

A. Calculation of Zero-Sequence Component in the Steady State

According to the aforementioned assumption that the grid is balanced and the power factor is unity, the instantaneous input currents are given by (8) with the voltages given in (7), where I_M is the amplitude of the phase current. The three-phase input currents of the rectifier can be shown as follows:

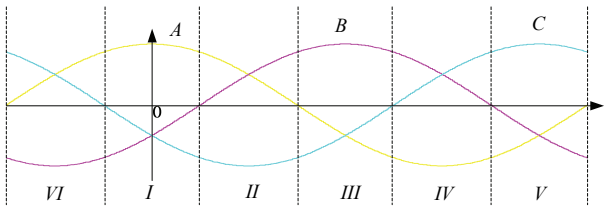

Fig. 4. Divisions of six sectors diagram.

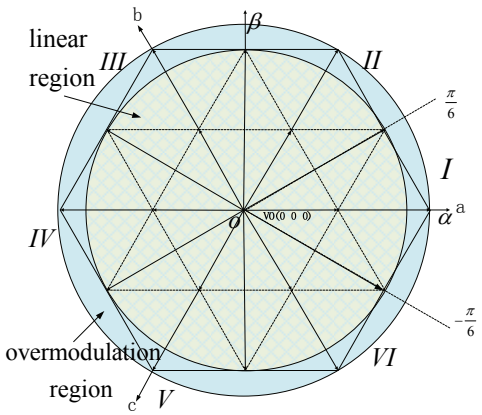

Fig. 5. Modulation region in space vector representation.

$$i_a = I_M\cos\omega t$$
$$i_b = I_M\cos(\omega t-2\pi/3) \quad (8)$$
$$i_c = I_M\cos(\omega t+2\pi/3)$$

In addition, for a three phase three wire system it follows that:

$$i_a+i_b+i_c=0 \quad (9)$$

If the zero-sequence component is injected into three phase sinusoidal modulation waves, the actual modulation waves can be given by:

$$v_a = v_{a0}+v_0$$
$$v_b = v_{b0}+v_0 \quad (10)$$
$$v_c = v_{c0}+v_0$$

For a three-level Vienna-type rectifier, which is current force commutated, the rectifier pole voltage is determined by the controlled switch state and the polarity of the ac phase current at the corresponding instance [13]. Due to the force commutation characteristics of the Vienna-type rectifier, the average neutral current in a modulation period can be obtained by:

$$i_{neu} = \sum_{x=a,b,c}(1-|v_x|)i_x = -\sum_{x=a,b,c}v_x|i_x|$$
$$= -v_{a0}|i_a|-v_{b0}|i_b|-v_{c0}|i_c|-v_0(|i_a|+|i_b|+|i_c|) \quad (11)$$

In the steady state, to implement the dc-link voltage balance, the neutral point injection current i_{neu} should always be zero in a modulation period. Therefore, from the voltage balance standpoint, the injected zero-sequence component should be controlled as:

$$v_0 = \frac{-v_{a0}|i_a| - v_{b0}|i_b| - v_{c0}|i_c|}{|i_a| + |i_b| + |i_c|} \tag{12}$$

For the unity power factor case, the input currents and voltages of each phase are in the same phase. Take $-\pi/6 \le \omega t \le \pi/6$ (section I) as an example. In this case, $|i_a| + |i_b| + |i_c|$ is equal to the absolute value of the maximum instantaneous ac input line current. Then the dc component of $|i_a| + |i_b| + |i_c|$ can be achieved by:

$$\frac{6}{T}\int_{-\frac{T}{12}}^{\frac{T}{12}} |i_a| + |i_b| + |i_c| dt = \frac{3}{\pi} I_M \tag{13}$$

with (7) and (8), the optimal zero-sequence component can be calculated as:

$$v_0 = \frac{m(1/2 - \cos 2\omega t)}{2\cos \omega t} \tag{14}$$

Consequently, the three-phase modulation waveform injected zero-sequence components can be calculated as:

$$\begin{aligned} v_a &= \frac{3}{4}\frac{m}{\cos \omega t} \\ v_b &= -\frac{\sqrt{3}}{2}\frac{m\cos(2\omega t + \pi/6)}{\cos \omega t} \\ v_c &= -\frac{\sqrt{3}}{2}\frac{m\cos(2\omega t - \pi/6)}{\cos \omega t} \end{aligned} \tag{15}$$

The calculation of zero-sequence components is the same when the reference vector is located in the other five sections. Thus, equation (16) can be obtained through the above analysis.

$$v_0 = \begin{cases} \dfrac{m(1/2 - \cos 2\omega t)}{2\cos \omega t} & \omega t \in \text{section}(I, III, V) \\ -\dfrac{m(1/2 - \cos 2\omega t)}{2\cos \omega t} & \omega t \in \text{section}(II, IV, VI) \end{cases} \tag{16}$$

B. Revising the Zero-Sequence Component for the Neutral-Point Voltage Balance

To solve this problem feedback control of the dc voltages is introduced to correct the disturbed voltage caused by a momentary disturbance. In addition, the upper capacitor and the lower capacitor in the dc-link have the same capacitance and characteristics, and this value is equal to C. Then the neutral-point voltage variation in a sample period can be calculated as:

$$\Delta v = V_{cp} - V_{cn} = -\frac{i_{\Delta v}}{C} T_s \tag{17}$$

where T_s is the sample period.

When there is a deviation of the neutral-point voltage, to balance the dc voltages in a sample period, the average neutral current, due to the voltage deviation between the upper capacitor and the lower capacitor, in a sample period should be controlled as:

$$i_{\Delta v} = -\Delta v C / T_s \tag{18}$$

The injected zero-sequence component should be revised as:

$$v_{0re} = \frac{-i_{\Delta v} - s_{\text{sgn}a} v_{a0} i_a - s_{\text{sgnb}} v_{b0} i_b - s_{\text{sgnc}} v_{c0} i_c}{s_{\text{sgn}a} i_a + s_{\text{sgnb}} i_b + s_{\text{sgnc}} i_c} \tag{19}$$

where $\left[s_{\text{sgn}a}, s_{\text{sgnb}}, s_{\text{sgnc}}\right]^T = \left[\text{sgn}(v_a), \text{sgn}(v_b), \text{sgn}(v_c)\right]^T$.

The signs of $v_x\,(x = a, b, c)$ are unknown before the zero-sequence component is calculated. For the Vienna-type rectifier, the algorithm can be further simplified since the grid voltages and line currents are in the same phase. In the analysis, $v_{\max 0} / v_{\max}$, $v_{\text{mid}0} / v_{\text{mid}}$ and $v_{\min 0} / v_{\min}$ are defined as the maximum, medium and minimum values of the three phase modulation waves with/without the injected zero-sequence component, and $i_{\max}$, i_{mid} and $i_{\min}$ are the currents of the corresponding phase. The injected zero-sequence component does not modify the relationship of the magnitude. Therefore, the new three phase modulation waves can be given by:

$$\begin{aligned} v_{\max} &= v_{\max 0} + v_0 \\ v_{mid} &= v_{mid0} + v_0 \\ v_{\min} &= v_{\min 0} + v_0 \end{aligned} \tag{20}$$

Three phase modulation waves with an injected zero-sequence component are set as $-1 \le v_x \le 1$, $x \in [\max, \text{mid}, \min]$. Thus, the span of the zero-sequence component that can be injected is expressed as:

$$-1 - v_{\min 0} \le v_0 \le 1 - v_{\max 0} \tag{21}$$

It is necessary to further analyze the relationship between the neutral current and the zero-sequence component. It is well known that $v_{\min} + v_{\text{mid}} + v_{\max} = 0$ and that there must be $v_{\min} < 0, v_{\max} > 0$. Only the sign of v_{mid} is not determined. However, whatever the sign is, v_{mid} and i_{mid} have the same phase and sign value. Thus, $v_{mid0}\,\text{sgn}(v_{mid}) i_{mid}$ can be simplified to $v_{mid0}|i_{mid}|$. The same approach can be applied to the other two phases to obtain the simplified form. The relationship between the neutral current and the revised zero-sequence component can be derived as follows.

$$v_0 = \frac{-i_{\Delta v} - v_{\max 0}|i_{\max}| - v_{mid0}|i_{mid}| - v_{\min 0}|i_{\min}|}{|i_{\max}| + |i_{mid}| + |i_{\min}|} \tag{22}$$

The substitution of (12), (13), (16) and (18) into (22) leads to the injected zero-sequence component as follows:

$$v_0 = \begin{cases} -\dfrac{\pi \Delta v C}{3 I_M T_s} + \dfrac{m(1/2 - \cos 2\omega t)}{2\cos \omega t} & \omega t \in \text{section}(I, III, V) \\ -\dfrac{\pi \Delta v C}{3 I_M T_s} - \dfrac{m(1/2 - \cos 2\omega t)}{2\cos \omega t} & \omega t \in \text{section}(II, IV, VI) \end{cases} \tag{23}$$

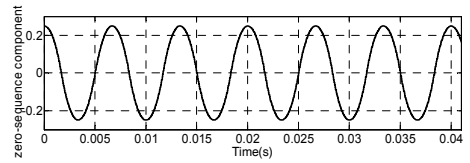

(a)

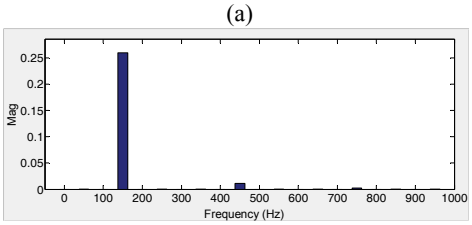

(b)

Fig. 6. Diagrams. (a) Waveform of v_0^*. (b) Spectrum of v_0^* ($m=1, \omega=314$).

Define equation (23) as:

$$v_0 = k\Delta v + v_0^* \tag{24}$$

where $k=-\pi C/3I_M T_s$. In addition, v_0^* is the optimal zero-sequence component in the steady state [13], and $k\Delta v$ is used to balance the dc-link voltage, which is called the controlled zero-sequence component.

Fig. 6(a) shows a waveform of the optimal zero-sequence component, and Fig. 6(b) shows spectrum analysis results for the case of m=1. v_0^*. This can be simplified as:

$$v_0^* \approx -0.259m\cos(3\omega t)+0.011m\cos(9\omega t) \tag{25}$$

The carried-based PWM method above is equivalent to the SVM method by injecting zero-sequence components. Additionally, there is a dc offset in the zero-sequence component v_0.

IV. Analysis of the Offset Extent with the Midpoint Potential Neutral Current

The SPWM method with zero-sequence components is equivalent to the SVM method. It is assumed that the grid is in the balanced state and that the PF is unity. Furthermore, the voltage loop is stable, and the neutral point is balanced. During every modulation period, if the rectifier system is in the steady state, to implement the neutral point voltage balancing control, the average neutral point current is controlled to zero. According to the operation features of Vienna-type rectifiers, the average neutral point current in every modulation is injected into middle-point of the dc-link output capacitors. This can be express as equation (5) in section III, which can be simplified as:

$$i_{neu} = \frac{1}{T_s}\int_{\gamma}^{\gamma+T_s}\sum_{k=a}^{c} d_k i_k dt \approx d_a i_a + d_b i_b + d_c i_c \tag{26}$$

where d_k is the duty ratio.

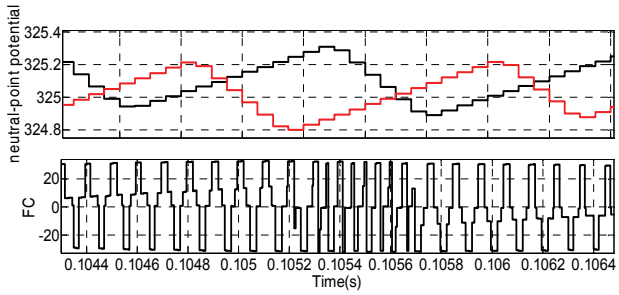

Fig. 7. The relationship between FC and the neutral-point potential.

If $v_{cp} > v_{cn}$, when the switch state $S_k(k=a,b,c)$ is on, and the relevant phase current $i_k(k=a,b,c)$ is negative (which means the current outflows from the midpoint of the dc-link capacitors), the midpoint potential unbalance extent is exacerbated by the relevant current. On the other hand, when the relevant phase current $i_k(k=a,b,c)$ is positive, the midpoint potential unbalance extent is suppressed by the relevant current. In the $v_{cp} < v_{cn}$ case, it has a similar analysis process with the above expression. It can be concluded from this analysis that the larger the current value $(|i_k|(k=a,b,c))$, the more notable the influence on the neutral-point potential. Here the factor of the neutral-point balance $(fn_k(k=a,b,c))$ is defined as:

$$fn_k = \frac{v_{cp}-v_{cn}}{|v_{cp}-v_{cn}|} i_k \quad k=a,b,c \tag{27}$$

Base on equations (26) and (27), the neutral-point voltage balance control factor (FC) is defined as follows:

$$FC = \sum_{k=a}^{c} fn_k d_k \quad k=a,b,c \tag{28}$$

In a modulation period, if $FC>0$, the average effect of the neutral-point current is an inhibition of the unbalance voltage offset. On the other hand, if $FC<0$, the midpoint potential unbalance extent is exacerbated by the neutral-point current. Furthermore, the larger the absolute value of FC, the more notable the influence on the neutral-point potential. The relationship between FC and the neutral-point potential is shown in the Fig. 7.

In addition, when the duty ratio changes to the switch state ($S_k \in \{0,1\}$; when the active switch is on, $S_k=1$; when the active is off, $S_k=0$), FC can express the influence on the neutral-point potential, which is carried out by any of the space vectors.

V. Simulation and Experimental Results

In this section, a detailed simulation has been built to verify the proposed control stagey on a SIMULINK platform. The circuit parameters used in the simulation model are listed in Table I.

TABLE I
SIMULATION PARAMETERS

RMS Source voltage	$220V$
Source frequency	$50Hz$
Input inductance L	$4mH$
Switching frequency	$15kHz$
DC link voltage	$650V$
Dc link capacitor	$2200\mu F$
Load resistance	50Ω

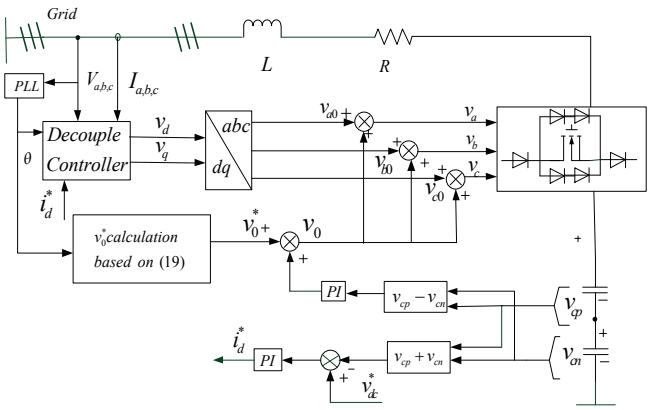

Fig. 8. Control block of SPWM with a zero-sequence component.

Fig. 8 shows a control block diagram of SPWM with a zero-sequence component, which can guarantee zero current injection into the neutral point. A decoupled controller, representing the standard two-level or three level multi-loop control topology in the synchronous reference frame (d-q frame) [19], [20], is commonly used to control the three phase boost rectifiers. In addition, the outer loop is designed for dc link voltage regulation. For the three-level neutral point clamping topology, an additional dc voltage balance loop is required. For the Vienna-type rectifier, used in this case instead of a complicated three-level space vector modulator, v_d and v_q are directly converted into the abc coordinates v_{a0}, v_{b0} and v_{c0} through an inverse Park's transformation. The dc link midpoint voltage balance is regulated by the zero sequence component v_0, which consists of two parts: a feed forward component v_0^*, and a feedback component ($k\Delta v$), where v_0^* is the optimal zero sequence given by (19).

When the modulation index m is set to 0.78, the corresponding modulation waveform with zero-sequence injection is shown in Fig. 9. Fig. 9(a) shows the A phase duty- cycle d_a and the zero-sequence component v_z. It can be seen that the simulation results are consistent with the theoretical analysis. Then Fig. 9(b) and (c) meet the operating characteristics of the three-level rectifier.

Fig. 10 shows steady-state and load-change waveforms of the Vienna rectifier. Fig. 10(b) shows that both the dc-link voltages and the ac input currents are well controlled. As a result, the power factor is close to unity. Furthermore, the

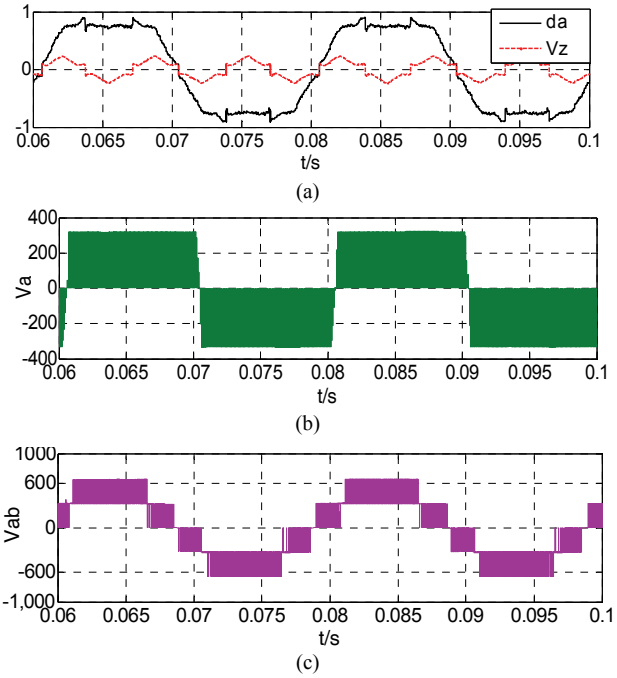

Fig. 9. Waveforms based on SPWM injected zero-sequence voltage (m=0.78). (a) A phase duty-cycle with a zero-sequence component. (b) v_a (phase voltage over switch). (c) v_{ab} (line voltage over switch).

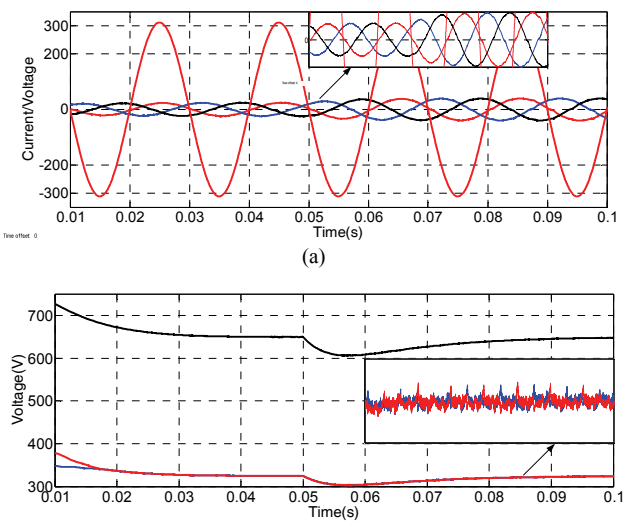

Fig. 10. Simulation results of the steady-state and a load change where the load resistance steps from 40 to 30 Ω. (a) Three phase currents i_a, i_b, i_c and source voltage u_a. (b) Full dc-link voltage v_{dc} and two capacitor voltages v_{cp}, v_{cn}.

neutral point voltage balance has been effectively controlled. In order to verify the dynamic performance, Fig. 10 shows the transient response for a load step-up case, where the load resistance steps from 40 to 30 Ω. The simulation results indicate that the proposed control approach is stable under load-step transient conditions. As can be seen, the neutral point voltage is effectively regulated by the zero sequence components.

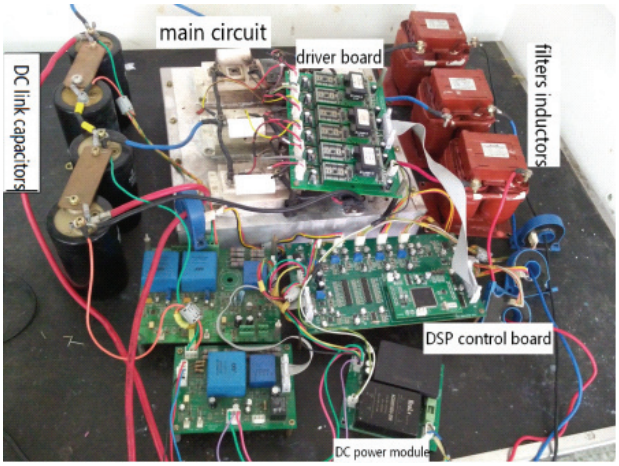

Fig. 11. Experimental system.

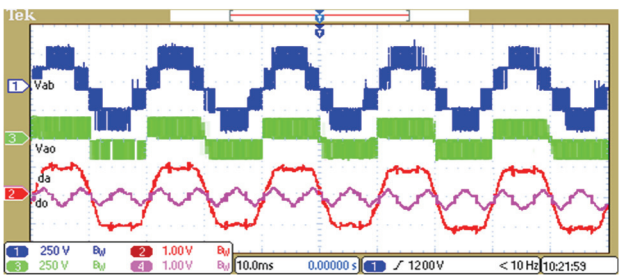

(a)

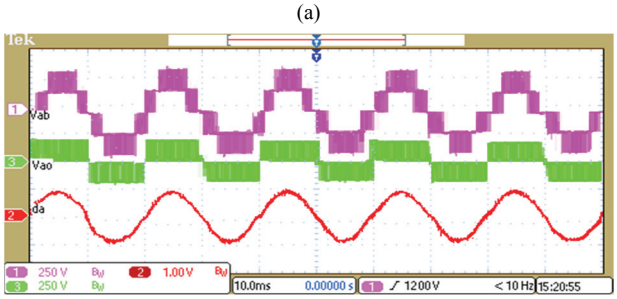

(b)

Fig. 12. Experimental waveforms of the SPWM. (a) SPWM with an injected zero-sequence voltage (m=0.78). (b) SPWM without a zero-sequence voltage.

To further illustrate and validate the proposed method, an experimental prototype is built at laboratory scale, which is shown in Fig. 11. A TMS320-F28335 DSP chip controller is used for sample control and to distribute the drive signals. The bidirectional switch is a SKM200GM12T4, the fast recovery diode is a IXYS DSEI2 101-12A. The input voltage is 220 Vrms/50Hz, the inductors are 4mH, and the switch frequency is 15 kHz. At the dc side, the two dc-link capacitors connected in series are 2200 and the load resister is 120. In addition, the dc reference voltage is 650V.

Figs. 12(a) and (b) show experimental results of the SPWM with a zero-sequence component algorithm and the SPWM algorithm. These wave-forms show the flexibility of the proposed the SPWM with a zero-sequence component algorithm, which agrees one-to-one with its corresponding space vector implementation. This was extensively verified through a

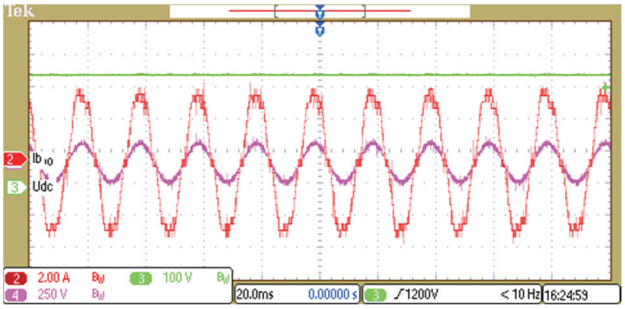

(a)

(b)

Fig. 13. Experimental results of the proposed control method. (a) B phase current and voltage waveform, and full dc-link voltage waveform in the steady-state. (b) Three-phase current harmonic distortions.

simulation analysis. Fig. 13(a) exhibits the phase b source voltage and phase b current steady-state waveforms of the proposed control method. As depicted in Fig. 3(a), the sinusoidal grid current and source voltage are exactly in phase, and the power factor value is about 0.99. Fig. 13(b) shows that the average THD is about 3.1%. This result confirms that the new modulation method is effective. Fig. 14 shows differential waveforms. Transient waveforms of the dc voltage and ac current are shown in the Fig. 14(a). At the same time, these waveforms can be used to depict the steady-state. Further illustrations of the relations between the ac current and ac source voltage are shown in Fig. 14(b) when the rectifier changes from the diode rectification mode to the active control mode. In addition, sinusoidal and symmetrical currents can be obtained and have the same phase angle as the respective source voltages. Fig. 14(c) shows that the neutral point voltage balance of the dc-link capacitors is well regulated by this method based on the simplified SVM. Fig. 14(d) shows the transient response for a load step-up case, where the load resistance steps from the disconnected state to the normal steady state.

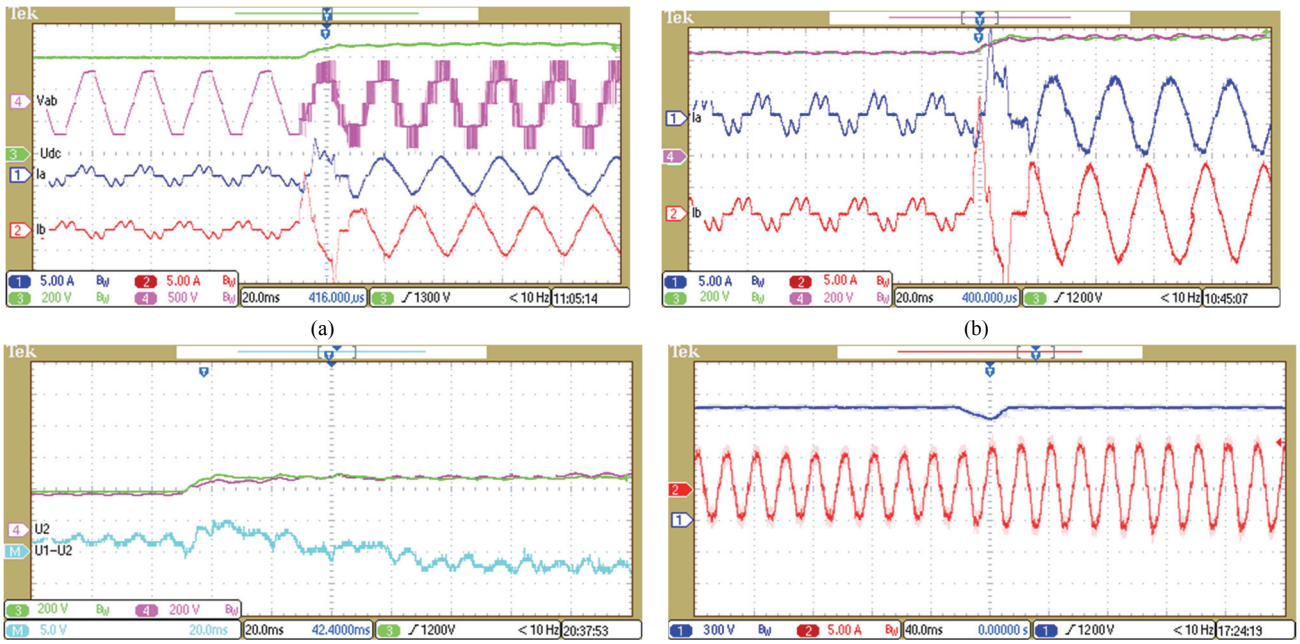

Fig. 14. Experimental waveforms. (a) Current and voltage form the start-up state to the steady state. (b) Current and voltage in the steady-state. (c) Voltage of the upper and lower capacitors, and subtraction of the upper and lower capacitor voltages. (d) A phase current and full dc-link voltage with the load resistance stepping from 120 to 75 Ω.

VI. Conclusion

This paper presents a SPWM with a zero-sequence component algorithm, which can significantly reduce the calculation effort and achieve very good performance in terms of the neutral point voltage balance. Additionally, the mechanism of the neutral point regulation is analyzed by precise zero sequence components. This paper also presents a comprehensive analysis of the relationship between the DC-Link neutral-point potential variation and the average current flowing out of or into the neutral point. Simulation and experimental results well match the theoretical analysis.

References

[1] J. W. Kolar and F. C. Zach, "A novel three-phase utility interface minimizing line current harmonics of high-power telecommunications rectifier modules," in *Proc. INTELEC '94*, pp. 367-374, 1994.

[2] H. Ma, Y. Xie, B. Sun, and L. Mo, "Modeling and direct power control method of vienna rectifiers using the sliding mode control approach," *J. Power Electron.,* Vol. 15, No. 1, pp. 190-201, Jan. 2015.

[3] H. Ma, Y. Xie, and Z. Shi, "Improved direct power control for Vienna-type rectifiers based on sliding mode control." *IET Power Electron.,* Vol. 9, No. 3, pp. 427-434, Mar. 2016.

[4] M. Zhang, B. Li, L. Hang, L. M. Tolbert, and Z. Lu, "Performance study for high power density three-phase Vienna PFC rectifier by using SVPWM control method," in *Proc. APEC*, pp. 1187-1191, 2012.

[5] H. Ma and Y. Xie, "A novel dual closed-loop control strategy based on sliding-mode variable structure of Vienna-type rectifier," *Transactions of China Electro- technical Society*, Vol. 28, No. 4, pp. 149-156, 2013.

[6] N. B. H. Youssef, F. Fnaiech, and K. Al-Haddad, "Small signal modeling and control design of a three-phase AC/DC Vienna converter," in *Proc. IECON*, pp. 656-661, Nov. 2003.

[7] R. Burgos, R. Lai, S. Rosado, F. Wang, D. Boroyevich, and J. Pou, "A full frequency range average model for Vienna-type rectifiers," in *Power Electronics Specialists Conference, 2008 IEEE*, pp. 4495-4502, Jun. 2008.

[8] J. W. Kolar and F. C. Zach, "A novel three-phase utility interface minimizing line current harmonics of high-power telecommunications rectifier modules," *IEEE Trans. Ind. Electron.*, Vol. 44, No. 4, pp. 456-467, Aug. 1997.

[9] N. Backman and R. Rojas, "Modern circuit topology enables compact power factor corrected three-phase rectifier module," in *Proc. INTELEC '02*, pp. 107-114, Oct. 2002.

[10] C. Qiao and K. M. Smedley, "Three-phase unity-power-factor star connected switch (VIENNA) rectifier with unified constant-frequency integration control," *IEEE Trans. Power Electron.*, Vol. 18, No. 4, pp. 952-957, Jul. 2003.

[11] H. Ma, W. Wei, L. Wang, and Z. Shi, "Research on SMC-predictive DPC strategy for Vienna rectifier," *IEICE Electronics Express.* Vol. 15, No. 19, pp. 1-9, 2018.

[12] L. Hang, B. Li, M. Zhang, Y. Wang, and L. M. Tolbert, "Equivalence of SVM and carrier-based PWM in three-phase/wire/level Vienna rectifier and capability of unbalanced-load control," *IEEE Trans. Ind. Electron.*, Vol. 61, No. 1, pp. 20-28, Jan. 2014.

[13] R. Lai, F. Wang, R. Burgos, D. Boroyevich, D. Jiang, and D. Zhang, "Average modeling and control design for Vienna-type rectifiers considering the DC-link voltage balance," *IEEE Trans. Power Electron.*, Vol. 24, No. 11, pp. 2509-2522, Nov. 2009.

[14] T. Viitanen and H. Tuusa, "Experimental results of vector

controlled and vector modulated Vienna I rectifier," in Proc. *IEEE PESC*, pp. 4637-4643, 2004.
[15] R. Lai, F. Wang, R. Burgos, and D. Boroyevich, "Voltage balance control of non-regenerative three-level boost rectifier using carrier-based pulse width modulation," *in Proc. IEEE PESC*, pp. 3137–3142, 2008.
[16] R. Burgos, R. Lai, Y. Pei, F. Wang, D. Boroyevich, and J. Pou, "Space vector modulator for Vienna-type rectifiers based on the equivalence between two- and three-level converters: A carrier-based implementation," *IEEE Trans. Power Electron.*, Vol. 23, No. 4, pp. 1888-1898, Jul. 2008.
[17] E. Robles, J. Pou, S. Ceballos, J. Zaragoza, J. L. Martin, and P. Ibanez, "Frequency-adaptive stationary-reference-frame grid voltage sequence detector for distributed generation systems," *IEEE Trans Ind. Electron.*, Vol. 58, No. 9, pp. 4275-4287, Sep. 2011.
[18] S. Qiang, L. Wenhua, Y. Qingguang, X. Xiaorong, and W. Zhonghong, "A neutral-point potential balancing algorithm for three-level NPC inverters using analytically injected zero-sequence voltage," in *Applied Power Electronics Conference and Exposition, 2003. APEC '03. 18th Annual IEEE*, pp. 228-233, 2003.
[19] M. Malinowski, M. Jasinski, and M. P. Kazmierkowski, "Simple direct power control of three-phase PWM rectifier using space vector modulation (DPC-SVM)," *IEEE Trans. Ind. Electron.*, Vol. 51, No. 2, pp. 447-454, Apr. 2004.
[20] B. Shi, G. Venkataramanan, and N. Sharma, "Design considerations for reactive elements and control parameters for three phase boost rectifiers," in *Electric Machines Drives, 2005. International Conference on*. pp. 1757-1764, 2005.

Hui Ma was born in Kaifeng, China, in 1985. He received his M.S. degree in Electrical Engineering and Automation from the Chang Chun University of Technology, Jilin, China, in 2013; and his Ph.D. degree in Power Electronics from the School of Electric Power, South China University of Technology, Guangzhou, China, in 2016. Since 2016, he has been an Assistant Professor in the College of Electrical Engineering and New Energy, China Three Gorges University, Yichang, China. His current research interests include high-power density rectifiers, multilevel converters, and electric energy conversion control strategies in various industrial fields. He served as a Reviewer for journals such as IET Power Electronics and the Journal of Power Electronics. He also served as a Reviewer at conferences such as the Annual Conference of the IEEE Industrial Electronics Society (IECON) and the IEEE Energy Conversion Congress & Exposition (ECCE).

Mao Feng was born in Chongqing, China, in 1993. She received her B.S. degree in Electrical Engineering from Chongqing Three Gorges University, Wanzhou, China, in 2016. She is presently working towards her M.S. degree in Electrical Engineering at China Three Gorges University, Yichang, China. Her current research interests include the energy management of hybrid fuel cells.

Yu Tian was born in Yichang, China, in 1996. He received his B.S. degree in Electronic Information Science and Technology from the Hubei University of Science and Technology, Xianning, China, in 2018. He is presently working towards his M.S. degree in Electrical Engineering at China Three Gorges University, Yichang, China. His current research interests include line loss analysis and management.

Xi Chen was born in Henan, China, in 1988. He received his M.S. degree in Pattern Recognition and Intelligent Systems from the College of Electronic and Information Engineering, Henan University of Science and Technology, Luoyang, China, in 2013; and his Ph.D. degree in Power Electronics from the School of Electric Power, South China University of Technology, Guangzhou, China, in 2018. His current research interests include the modeling and control of nonlinear systems. He served as a Reviewer of journals such as IEEE Transactions on Circuits and Systems-II: Express Briefs, Nonlinear Dynamics, Mechatronics and IEEE Access.